Phys. Status Solidi A **206**, No. 5, 976–979 (2009) / **DOI** 10.1002/pssa.200881294

physica status solidi a
www.pss-a.com
applications and materials science

Optical properties of thick metal nanohole arrays fabricated by electron-beam and nanosphere lithography

Ahmad Reza Hajiaboli[*,1], **Bo Cui**[2], **M. Kahrizi**[1], **and Vo-Van Truong**[3]

[1] Electrical and Computer Engineering, Concordia University, 1455 de Maisonneuve Blvd. West, Montréal, Canada
[2] Industrial Materials Institute, National Research Council of Canada (NRC), Boucherville, QC, Canada
[3] Department of Physics, Concordia University, 1455 de Maisonneuve Blvd. West, Montréal, QC, Canada

Received 29 August 2008, revised 18 October 2008, accepted 22 October 2008
Published online 22 April 2009

PACS 36.20.Ng, 42.50.St, 73.20.Mf, 81.16.Nd, 82.45.Yz

[*] Corresponding author: e-mail ahmad.hajiaboli@ieee.org, Phone: +001 514 739 6640, Fax: +001 514 6640

Optically thick metallic nanohole structures were fabricated using two different methods – electron-beam and nanosphere lithography. The nanosphere lithography technique was based on self-assembling of polystyrene or silica nanospheres (0.560–1.25 μm in diameter) followed by the deposition of a silver film. The holes size and periodicity of the patterns as well as optical properties (transmission and reflection in the Visible–NIR) of the structures were investigated. The extraordinary optical transmission (EOT) was studied experimentally in both structures and it was found to be dependent on the geometrical parameters (holes shape, diameter and periodicity of structures). As the samples were made for long range order, the effect of the defects like missing holes, change of periodicity or variation of the holes shape, were also studied. The experimental results, especially the position of the SPR band in the different nanohole structures, were compared with those found by simulation carried out with 3D FDTD (finite difference time domain).

1 Introduction Studies reported by Ebbesen and coworkers in 1998 indicate that the light transmission through a periodic array of sub-wavelength holes in an optically thick metallic film can be several orders of magnitude higher than that expected in the classical Bethe's theory [1–3]. Extraordinary optical transmission (EOT) through nanohole arrays has been studied extensively in several aspects, including the theory and evidence of its origin [4, 5] parameters affecting its intensity, the optical properties such as its transmission spectra and divergence. Although it is still not universally accepted [6], EOT is explained as a result of resonant coupling between incident light and collective oscillation of electrons, surface plasmon resonance (SPR) at the metal-dielectric interface, through nanohole arrays [7].

Several parameters including the refractive index of the medium on the metal film surface, the wavelength and state of polarization of the incident light, the holes shape and periodicity of the structures change the spectral behaviour in term of intensity and position of the transmitted peaks. The structures that support EOT have found their applications in many fields including visible spectroscopy [8], Raman spectroscopy [9], sub-wavelength optics [10], nonlinear optics [11], and photolithography [12].

Since EOT is in part determined by the refractive index of the medium on the metal film surface, one could use EOT to monitor the surface refractive index, which is directly related to the physical and chemical properties of the material on the surface. This concept prompted much research that studied surface chemical or physical reactions on a metal film based on either the intensity or spectra of EOT through nanohole arrays sensors. Functioning as biosensors, nanohole arrays have several unique advantages over the other type of SPR-based biosensors including higher density of the sensors even with a small array of nanoholes, simpler instruments for the transmission light measurements. As the EOT is affected by parameters like the shape and periodicity of the holes, devices made based on this phenomenon will be more sensitive and supports larger selectivity. In spite of all these advantages most of

existing application of EOT has been realized on the structures with limited area of coverage [13]. Due to the limited techniques and options for fabrication of such structures, the EOT-based devices were fabricated with finite array sizes. If the array contains a small number of holes, the periodicity is not well defined and the contribution from edges becomes significant, changing the spectrum and leading to unusual re-emission patterns [7].

In long range order nanohole structures, the effect of the periodicity of the structures becomes more dominant in the optical properties of the device. Contribution of diffracted surface waves will become more important in presence of long range order array of holes [14].

In this paper, we demonstrate two methods that can produce arrays of nanoholes with sizes of 100–300 nm over large areas of the thick metallic films. One of the techniques, using nanosphere lithography, is reported for the first time. The 3D FDTD simulation is also presented, which exhibits a good agreement with the experimental results of optical photo spectrometry in the UV–VIS range. Analyses of results show that the fabricated structures are a good candidate for SPR-based biosensors.

The rest of the paper is organized as the following: in Section 2, two methods of fabrication are presented and the geometry and the quality of the fabricated structures are characterized. The experimental results of the optical measurements are shown in Section 3. In Section 4, the simulation results of the structures are presented. Finally, this paper is concluded with highlighting some remarks in Section 5.

2 Fabrication methods

2.1 Electron beam lithography (EBL) A double lift off technique has been developed to address the fabrication of the planar nanoholes array in long range order on thick metallic films.

The method is optimized for the fast and the high resolution outcomes. A modified scanning electron microscopy (SEM) is used to write the pattern on the ZEP-520, a recently introduced polymer as electron resist material, which supports up to three times faster scanning rate compared to the more commonly used polymer, Polymethyl methacrylate (PMMA).

The recipe is divided to six steps as follows:

(I) A stack up structure consists of layers of Polydimethylglutarimide (PMGI) and titanium (Ti) covered by a layer of ZEP-520. It is prepared using spin coating for depositing the polymer layers and electron beam evaporation for the metallic layer of Ti.

(II) The pattern of the holes is written on the direct electron resist of ZEP-520 using the modified SEM. The acceleration voltage is set to 10 kV and the scanning is adjusted for 50 us exposure of electron on each spot. The Ti layer below the polymer serves as a metallic layer for electron discharge from the surface to decrease the distortion of the beam gun and protect the PMGI layer from exposure.

Table 1 RIE of polymers and silica.

material	etchant	flow rate	etching rate
polystyrene	O_2	20	35 nm
silica/Ti	CHF_3/O_2	20/2	65/5 nm
PMGI	O_2	20	85 nm

(III) The pattern is developed by immersing the sample in the xylene solution for 20 minutes. Then a thin layer of chromium (Cr) is deposited on the sample.

(IV) The first lift off is going to leave the arrays of the dots on the planar surface of Ti. The lift off is done by immersing the sample in a solution of anisole and sonication for 25 minutes.

(V) Reactive ion etching RIE is used to remove the Ti and the PMGI. Ti layer is etched using the mixture of the gases as O_2/CHF_3 by the flow rate of 2/20 sccμm. This step is done for 1:30 minutes and the next step to remove polymer was done with only oxygen as etchant for 2.5 minutes. The detail of RIE conditions for different materials appears in the Table 1.

The results at this step are a pillar structure formed by the PMGI polymer and Ti and Cr layers. Metallization should take place by evaporation of gold or silver on the pillar structures.

(VI) Lift off by PMGI and formation of the nanoholes array by immersing the sample into the NH_3OH for 20 minutes in the last step. PMGI is then removed from the substrate, leaving the holes open in the metal film.

Figure 1 shows the circular shape of holes fabricated by EBL. The holes are arranged in the face-centred cubic (FCC) array, which is not possible to be fabricated by NSL.

The use of ZEP-520 as electron beam resist reduces the writing time by an order of 3 times compared to the PMMA. On the other hand, the perforated holes are not perfectly circular which due to the lower resolution obtained by this polymer.

As the writing beam reaches the boundaries of the scanning region, the beam becomes out of focus resulting

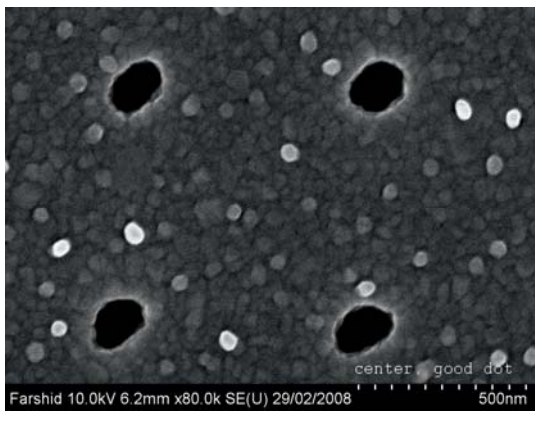

Figure 1 SEM image of the nanohole structures. The close up image shows that holes are not perfectly circular.

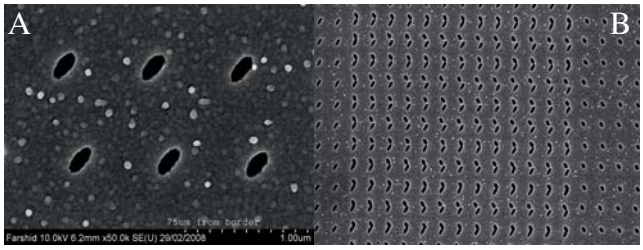

Figure 2 A) Pattern area at the border of the scanning region where holes become elliptical. B) The result obtained in the case of overlapping of the unit areas.

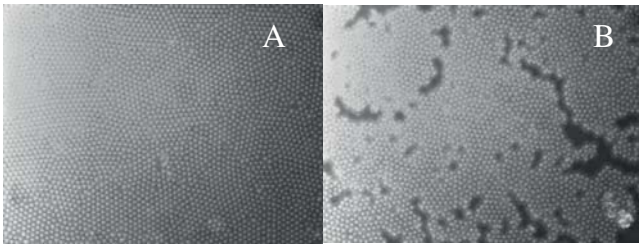

Figure 3 Optical images of the templates of microspheres deposited into 2D crystalline structures A) silica 1.2 μm, B) polystyrene 750 nm.

in the formation of elliptical holes rather than circular holes. To resolve this problem, the whole scanning region is divided into several unit areas of 400 μm by 400 μm. The beam of electrons is refocused in each of these unit areas so that the uniformity is more preserved throughout the entire structure. A drawback of this technique is the overlapping of these unit areas as shown in Fig. 2(B).

2.2 Nanospheres lithography (NSL) A low-cost and high throughput process for the realization of 2D arrays of deep sub-wavelength features using a self-assembled monolayer of hexagonally close packed (HCP) silica or polystyrene microspheres is presented. This method utilizes the microspheres as template to fabricate nanohole structures with a high aspect ratio over large areas on glass substrates. The period and diameter of the holes formed with this technique can be controlled precisely and independently.

The microsphere colloidal crystal has been used for more than a decade in many applications such as photonic crystals. The formation of the multilayer colloidal crystal has been proposed by many techniques such as drop coating vertical deposition and has been presented in reference [15] where we demonstrate a new method for self assembled crystallization of multilayer micro-spheres in long range order called the "flow control" method. The monolayer deposition of the microsphers is a more challenging task due to the fact that the microspheres suspended in the colloidal solution will easily form 3D crystalline structures during the process of crystallization rather than being distributed evenly on the substrate to form a 2D crystal.

The NSL method is divided into four steps as follows:

(I) The substrate is cleaned using Prinha and dried by N_2 and a monolayer microspheres of either silica or polystyrene is deposited using spin coater. Coating is done at a 750 RPM spin rate which is determined empirically as the optimum speed for the original concentration of 5% of the microspheres of polystyrene (750 nm in diameter) and silica (1.2 μm). The images of these templates obtained by optical microscopy are shown in Fig. 3.

(II) Etching of the spheres using RIE. The rate of etching and conditions for etching of polystyrene or silica can be found in Table 1. The diameter of the spheres after the etching will determine the diameter of the holes in array. The periodicity is imposed by the diameter of spheres before etching. RIE of silica and polystyrene microspheres is an anisotropic process i.e. the etching rate in the vertical direction is more than the one in the lateral directions. Thus, the shrinkage of the size of the holes will occur when the spheres are etched more than half of their height.

(III) Metallization of the substrate using electron beam evaporation. First a thin layer of Cr is deposited on the substrate and the layer is covered by 100 nm to 150 nm of gold or silver. The Cr layer serves as an intermediate layer to increase adhesion between silver or gold and the glass substrate.

(IV) Removing the spheres from the structure will leave the holes open in the structure. Sonication of the sample in ethanol will dissolve the polystyrene spheres and remove them from the substrate. The silica spheres are not dissolved in solvent or alcohols however, the mechanical forces applied to the sample during sonication would contribute to the process of removing the silica spheres. The removing the silica spheres from the substrate required more than 30 minutes of sonication.

The perfectly circular hole arrays shown in Fig. 4 are the result of the NSL fabrication. As it is mentioned before, during the RIE, spheres, regardless of their material, whether they are silica or polystyrene, are submitted to an anisotropic etching process. Thus, maintaining enough height of the spheres (in the order of 100 nm) for the next two steps of fabrication (i.e. metallization and spheres removal from the template) is challenging, specially for

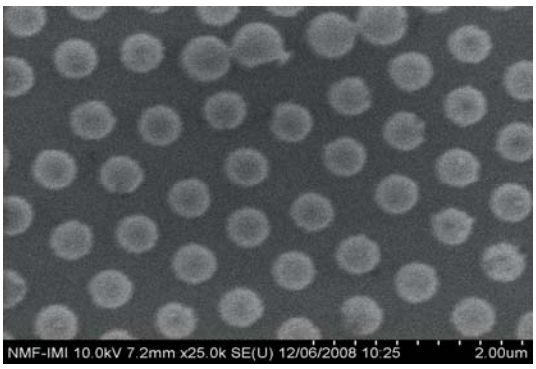

Figure 4 SEM image of the nanoholes array fabricated by NSL. Metal thickness is (8/60) nm of Cr/Ag.

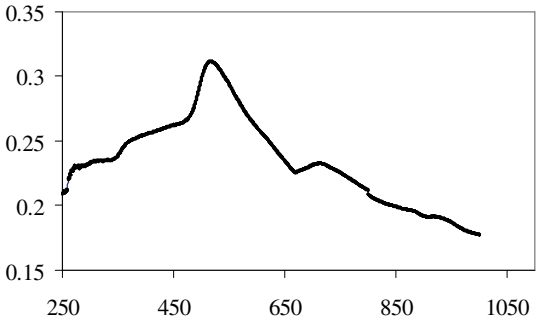

Figure 5 Transmission spectrum of the 650 nm nanoholes array peak (transmission coefficient, vertical axis, versus wavelength).

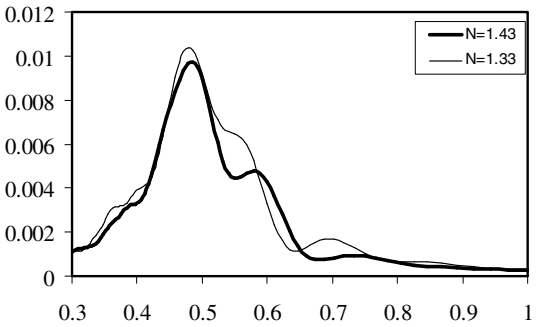

Figure 6 FDTD simulation of transmission spectrum. The red shift in the peak position is due to the change in the ambient index of refraction from 1.3 to 1.4.

small holes. So far, the holes with sizes of 200 nm to 300 nm have been successfully fabricated by this technique.

3 Characterization – optical spectrometry The transmission spectrum of the structures has been characterized by a UV–VIS spectrometer 'Cary 5000' from Varian.

Figure 5 shows the transmission spectrum of the gold nanohole structure with periodicity of 650 nm and holes diameter of 100 nm. The film thickness is 120 nm and the structure is fabricated on a glass substrate. The first peak structure located near 530 nm would be associated with the bulk properties of gold. The second peak at longer wavelengths located at 680 nm would be associated to the surface plasmon excitation on the metal surface as related to the interaction of light with the periodic structures, and can be tailored by changing the nanohole periodicity.

4 Simulation A numerical calculation for the field distribution has been carried out using a commercial FDTD package by Optiwave called OptiFDTD. Optical properties of gold have been modelled using the so-called Lorentzian-Drude model. The numerical calculation results are compared to the experimental results obtained by the UV–VIS photo spectroscopy. The 3D-FDTD simulation results shown in Fig. 6 are the transmission spectrum for a structure with a periodicity of 650 nm and a hole diameter of 100 nm. The thick line shows the spectrum when the structure is exposed to an environment with a refraction index of 1.43 whereas the thin line depicts the spectrum when the ambient refraction index is 1.33. A shift in the spectrum is clearly demonstrated. The first peak in the spectrum is related to the material properties of the metallic nanostructures and has not been affected by the change in the surrounding medium. On the other hand, the second and the third peaks are very sensitive to the little change in refractive index of the environment in contact with the structures.

The sensitivity of the second and the third peak have been determined to be as following:

$$s_2 = 460 \times 10^{-8}\ \text{RIU}, \qquad s_3 = 800 \times 10^{-8}\ \text{RIU}.$$

These values are found to be particularly high, suggesting the potential biosensing applications of the fabricated structures.

5 Conclusion Two methods of fabrication for long range periodic nanohole structures have been developed. The methods have been evaluated in terms of their limitation and quality of the fabricated structures. Structures obtained by these techniques allow their optical characterization by conventional UV–VIS photo-spectroscopy. Simulation and experimental results are in good agreement. In particular the strong dependence on the ambient index of refraction is clearly demonstrated in the simulation results.

Acknowledgements The financial support for this research is partially provided by the Natural Science and Engineering Research Council of Canada (NSERC). We thank Dr. Teodor Veres in CNRC-IMI Laboratories and Dr. Kalman in Physics Department at Concordia University for their support.

References

[1] T. W. Ebbesen et al., Nature **391**(6668), 667–669 (1998).
[2] H. A. Bethe, Phys. Rev. **66**(7/8), 163 (1944).
[3] D. E. Grupp et al., Adv. Mater. **11**(10), 860–862 (1999).
[4] A. Degiron and T. W. Ebbesen, J. Opt. A **7**(2), S90–S96 (2005).
[5] V. Lomakin and E. Michielssen, Phys. Rev. B **71**(23), 235117-10 (2005).
[6] H. J. Lezec and T. Thio, Opt. Express **12**(16), 3629 (2004).
[7] C. Genet and T. W. Ebbesen, Nature **445**(7123), 39–46 (2007).
[8] J. V. Coe et al., Annu. Rev. Phys. Chem. **59**(1), 179–202 (2008).
[9] A. G. Brolo et al., Nano Lett. **4**(10), 2015–2018 (2004).
[10] W. L. Barnes et al., Nature **424**(6950), 824–830 (2003).
[11] J. A. H. van Nieuwstadt et al., Phys. Rev. Lett. **97**(14), 146102-1 (2006).
[12] X. Luo and T. Ishihara, Opt. Express **12**(14), 3055–3065 (2004).
[13] A. G. Brolo et al., Langmuir **20**(12), 4813–4815 (2004).
[14] T. Rindzevicius et al., J. Phys. Chem. C **111**(3), 1207–1212 (2007).
[15] S. Badilescu et al., J. Mater. Sci., Mater. Electron. **18**, S383–S387 (2007).